JACS
JOURNAL OF THE AMERICAN CHEMICAL SOCIETY
Article
pubs.acs.org/JACS

A Potent and Site-Selective Agonist of TRPA1

Junichiro Takaya,[†,‡] Kazuhiro Mio,[∥] Takuya Shiraishi,[⊥] Tatsuki Kurokawa,[⊥] Shinya Otsuka,[§] Yasuo Mori,[⊥,#] and Motonari Uesugi*[,‡,§]

[†]Graduate School of Medicine, Kyoto University, Kyoto, Kyoto 606-8501, Japan

[‡]Institute for Chemical Research and [§]Institute for Integrated Cell-Material Sciences (WPI-iCeMS), Kyoto University, Uji, Kyoto 611-0011, Japan

[∥]Molecular Profiling Research Center for Drug Discovery, National Institute for Advanced Industrial Science and Technology, Koto-ku, Tokyo 135-0064, Japan

[⊥]Department of Synthetic Chemistry and Biological Chemistry, Graduate School of Engineering, and [#]Department of Technology and Ecology, Hall of Global Environment Studies, Kyoto University, Nishikyo-ku, Kyoto 615-8510, Japan

Supporting Information

ABSTRACT: TRPA1 is a member of the transient receptor potential (TRP) cation channel family that is expressed primarily on sensory neurons. This chemosensor is activated through covalent modification of multiple cysteine residues with a wide range of reactive compounds including allyl isothiocyanate (AITC), a spicy component of wasabi. The present study reports on potent and selective agonists of TRPA1, discovered through screening 1657 electrophilic molecules. In an effort to validate the mode of action of hit molecules, we noted a new TRPA1-selective agonist, JT010 (molecule **1**), which opens the TRPA1 channel by covalently and site-selectively binding to Cys621 (EC_{50} = 0.65 nM). The results suggest that a single modification of Cys621 is sufficient to open the TRPA1 channel. The TRPA1-selective probe described herein might be useful for further mechanistic studies of TRPA1 activation.

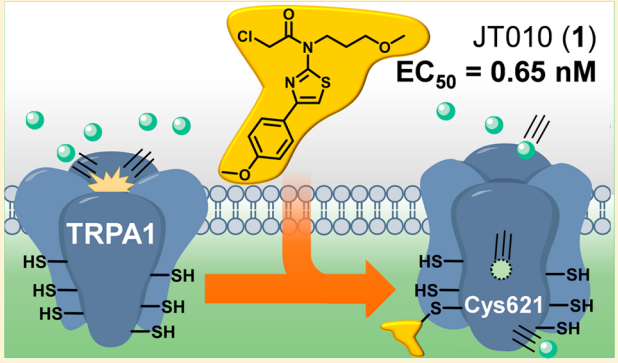

INTRODUCTION

The transient receptor potential (TRP) channel superfamily comprises a diverse group of cation channels that mediate a variety of physiological processes.[1,2] Among the members, the TRPV1 and TRPA1 channels sense endogenous algesic substances and environmental irritants, evoking defensive responses, such as pain, coughing, and changes in respiration pattern.[3−6] Because of their involvement in nociception, TRPV1 and TRPA1 have been targets for the development of novel pain reducers.[7,8]

TRPA1 senses broader environmental stimuli than TRPV1, including cold,[9] abnormal pH,[10−13] zinc,[14] and reactive irritants.[15−17] The best recognized agonist of TRPA1 is allyl isothiocyanate (AITC), a spicy component of wasabi.[18] Electrophilic molecules, including AITC, react covalently with multiple cysteine residues of TRPA1, causing conformational change that opens the channel.[15,16] Site-directed mutagenesis studies have identified three cysteines within the cytoplasmic NH_2-terminus of human TRPA1 (Cys621, Cys641, and Cys665), whose simultaneous mutation negates the channel-activating effects of several electrophilic reagents.[15] On the other hand, mass spectrometric analysis has revealed three cysteines on mouse TRPA1 (Cys415, Cys422, and Cys622) as target sites for electrophilic agonists.[16] Those target sites are conserved in the human homologue of TRPA1 (Cys414, Cys421, and Cys621).

Despite these insights, it remains unclear how the modification of multiple cysteine residues leads to the activation of TRPA1. The present study reports the discovery and analysis of a new potent, TRPA1-selective agonist. JT010 (molecule **1**), a thiazole derivative equipped with a chloroacetyl group, binds covalently and selectively to a single cysteine, Cys621, to open the TRPA1 channel (EC_{50} = 0.65 nM). The site-selective chemical probe described herein might serve as a tool for further mechanistic studies of TRPA1 activation.

RESULTS

Screening of Electrophilic Molecules. TRPA1 is generally thought to be activated by reactive molecules, including electrophilic compounds. To identify potent, selective agonists of TRPA1, we screened a chemical library of 1657 moderately electrophilic molecules that contain chloroacetyl, bromoacetyl, or epoxide groups (Figure S1A−D). The molecules were screened to identify agonists that cause a calcium influx in TRPA1-transfected HEK293 cells. The calcium influx was estimated by measuring signals from Fluo-

Received: September 28, 2015
Published: December 2, 2015

DOI: 10.1021/jacs.5b10162
J. Am. Chem. Soc. 2015, 137, 15859−15864

8, a fluorescent Ca^{2+}-indicator dye. Three structurally related molecules induced a calcium influx at half-maximal effective concentrations (EC_{50}) less than 1 nM (Figure S1E). These hit molecules share a 2-chloro-*N*-(thiazol-2-yl)acetamide structure (Figure S1F). We selected one of the three molecules, 2-chloro-*N*-(4-(4-ethoxyphenyl)thiazol-2-yl)-*N*-(3-methoxypropyl)-acetamide (JT010; molecule **1** in Figure 1A), for further investigation.

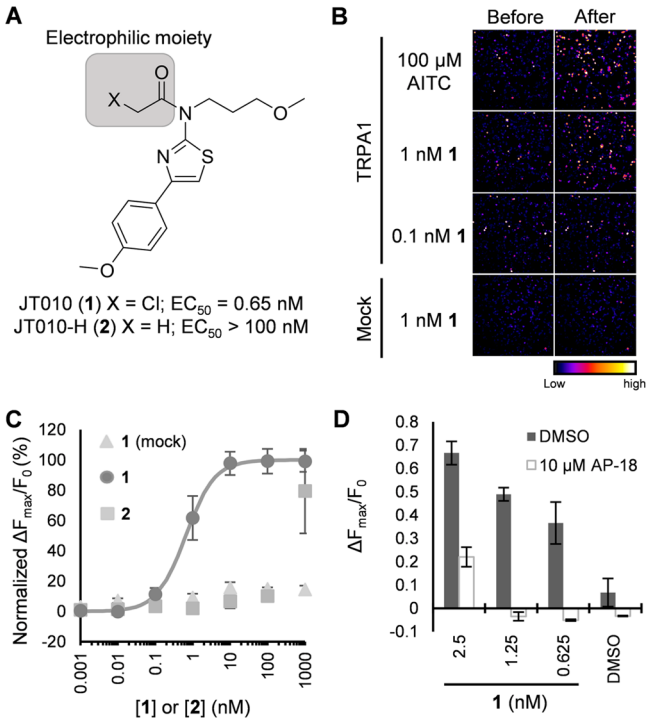

Figure 1. Molecule **1** stimulates calcium influx through the TRPA1 channel. (A) Chemical structures of JT010 (**1**) and its nonelectrophilic derivative, JT010-H (**2**). (B) Representative calcium images analyzed for response of Fluo-8-loaded TRPA1- or mock-transfected HEK293 cells to molecule **1** or AITC. (C) Dose–response curve of Fluo-8 fluorescence changes induced by molecule **1** or **2** in TRPA1- or mock-transfected cells. Fluorescence changes ($\Delta F_{max}/F_0$) were normalized to the maximum response induced by molecule **1**. The plots were fitted to a four-parameter logistic model, using ImageJ. An EC_{50} of 0.65 nM was calculated from the fitted curve. Data points are mean ± s.e.m. (n = 3). (D) The inhibitory effect of AP-18 on Fluo-8 fluorescence changes induced by molecule **1** in TRPA1-transfected HEK293 cells. 10 μM AP-18 or DMSO (control) was added to the cells prior to activation of TRPA1 by molecule **1** at the various concentrations. Data points are mean ± s.d. (n = 2).

Molecule 1 as a Potent Electrophilic Agonist of TRPA1. The chemical structure of molecule **1** was confirmed by its chemical synthesis (Scheme S1) and TRPA1 activity (Figure 1A–C). Calcium imaging assays demonstrated that 1 nM of synthesized molecule **1** caused calcium influx at comparable levels to 100 μM AITC in cells overexpressing TRPA1 but caused no detectable activity in the mock-transfected cells (Figure 1B). The effect of molecule **1** is dose-dependent, with an EC_{50} value of 0.65 nM (Figure 1C). In contrast, JT010-H (**2**), a derivative of molecule **1** in which Cl is replaced with H, displayed activity ~1000 times weaker (EC_{50} > 100 nM), indicating the importance of the electrophilic functional group of molecule **1**. It is likely that molecule **1** reacts with cysteine residues in TRPA1, similarly to other electrophilic agonists, including AITC.

To confirm that the calcium influx activity of molecule **1** is TRPA1-dependent, we examined the effects of AP-18 and HC-030031, selective antagonists of TRPA1,[19,20] on the activity of molecule **1**. As expected, AP-18 (10 μM) suppressed calcium influx stimulated by molecule **1** in cells overexpressing TRPA1 (Figure 1D). The inhibitory effect of AP-18 and HC-030031 was dose-dependent, with IC_{50} values of 9.1 and 10.3 μM, respectively (Figure S2).

Selectivity of Molecule 1 among TRP Channels. Known TRPA1 agonists often activate TRP channels other than TRPA1. For example, SNAP, an NO donor, potentiates TRPA1, TRPV1, TRPV3, TRPV4, and TRPC5;[21,22] H_2O_2 stimulates TRPA1, TRPM2, and TRPC5;[23,24] L-menthol evokes TRPA1, TRPV3, and TRPM8;[25] and isothiocyanates, including AITC, activate TRPA1, and TRPV1.[26−28] Calcium imaging assays with HEK293 cells that express all seven of the selected TRP channels showed that molecule **1** is highly selective for TRPA1 (Figure 2). TRPV1, TRPV3, TRPV4, TRPM2, TRPM8, and TRPC5 were not activated, even with 1 μM of molecule **1**.

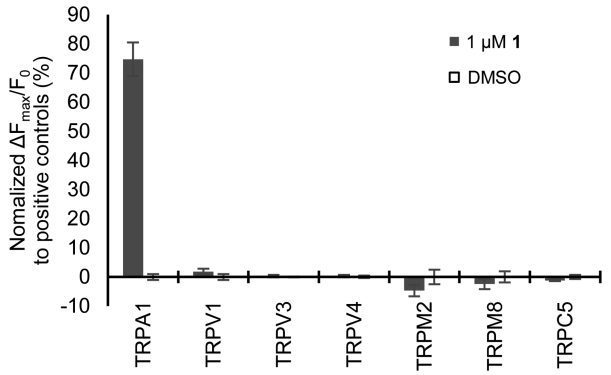

Figure 2. Among TRP channels, molecule **1** selectively affects TRPA1. Fluo-8 fluorescence changes stimulated by 1 μM molecule **1** or DMSO (control) in TRPA1-, TRPV1-, TRPV3-, TRPV4-, TRPM2-, TRPM8-, or TRPC5-transfected HEK293 cells. Fluorescence changes were normalized to the following positive controls: TRPA1 to 100 μM AITC; TRPV1 to 10 μM capsaicin; TRPV3 and TRPV4 to 50 μM 2-APB; TRPM2 to 1 mM H_2O_2; TRPM8 to 100 μM L-menthol; TRPC5 to 30 μM DTNP. Data points are mean ± s.e.m. (n = 3).

Covalent Interaction of Molecule 1 with TRPA1. To confirm the covalent interaction of molecule **1** with TRPA1, we chemically synthesized molecule **3**, a biotinylated analogue of molecule **1** (Figure 3A and Scheme S2). Molecule **3** retained a nanomolar range activity (EC_{50} = 30 nM), although its activity was ~50 times weaker than that of molecule **1** (Figure 3B).

Molecule **3** was incubated for 10 min with cells over-expressing TRPA1 fused with EGFP at the NH_2 terminus. After extensive washing, the cells were lysed, and the proteins that reacted with molecule **3** were purified using avidin agarose beads. Western blot analysis with an EGFP antibody visualized the biotinylated EGFP–TRPA1 in a dose-dependent manner (Figure 3C). When mock-transfected cells were used, no bands were detected. Moreover, competition with excess amounts of molecule **1** impaired the biotinylation of EGFP–TRPA1 (Figure 3D). When similar experiments were performed with an antibody against TRPA1 instead of the EGFP antibody, essentially the same results were obtained (Figure S3).

DOI: 10.1021/jacs.5b10162
J. Am. Chem. Soc. 2015, 137, 15859–15864

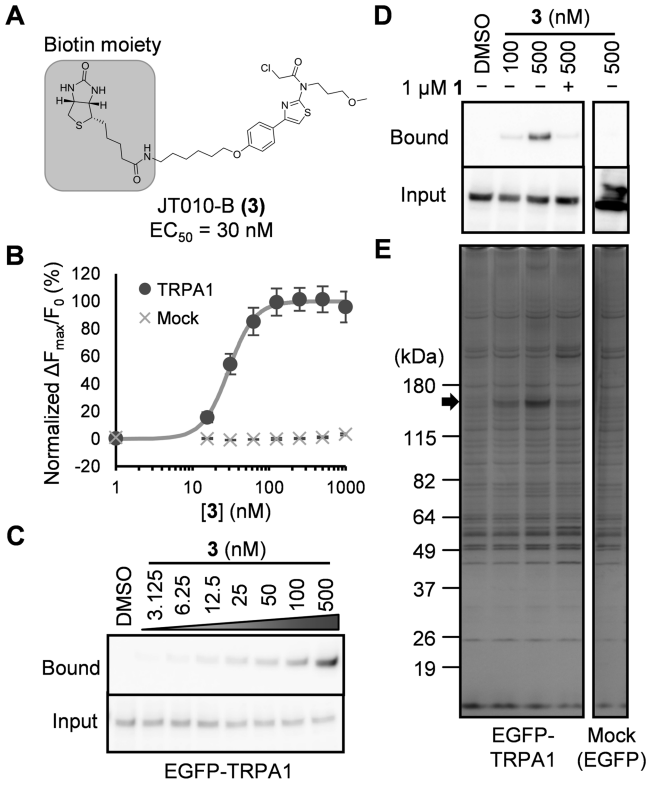

Figure 3. Selective biotinylation of TRPA1 by molecule **3**. (A) Chemical structure of molecule **3** (JT010-B), a biotinylated derivative of molecule **1**. (B) Dose–response curve for molecule **3**-induced Fluo-8 fluorescence changes in TRPA1- or mock-transfected cells. Fluorescence changes were normalized to the maximum response induced by molecule **3**. The plots were fitted to a four-parameter logistic model, using ImageJ. An EC_{50} value of 30 nM was calculated from the fitted curve. Data points are mean ± s.e.m. (n = 6–15). (C) Dose-dependent biotinylation of EGFP-TRPA1 by molecule **3**. EGFP-TRPA1-transfected HEK293 cells were incubated for 10 min with molecule **3** or DMSO (control) at various concentrations, and biotinylated proteins were purified using avidin beads. Purified samples (bound) and cell lysate (input) were analyzed by Western blot analysis with EGFP antibody. (D) Molecule **1** prevents biotinylation of EGFP-TRPA1 by molecule **3**. EGFP-TRPA1- or mock (EGFP)-transfected cells were treated with molecule **1** and/or **3** at the various conditions, and biotinylated proteins were purified and analyzed by Western blot analysis. (E) SDS-PAGE analysis with silver staining of an aliquot of the samples in (D). Arrow indicates a single band at ∼160 kDa that is dependent on molecule **3**.

An aliquot of the samples was also analyzed by SDS-PAGE analysis, and the proteins in the gel were visualized by silver staining (Figure 3E). Many bands were detected on the gel, possibly due to the presence of endogenous biotinylated proteins and nonspecific proteins. However, we observed a single band at ∼160 kDa that is dependent on molecule **3**, consistent with the size of the EGFP–TRPA1 fusion protein. The intensity of this band was reduced, when the cells were coincubated with excess amounts of molecule **1**, or when mock-transfected cells were used.

To confirm the irreversible reaction of molecule **3** with TRPA1, we carried out another biotinylation experiment. Cells overexpressing EGFP–TRPA1 were pretreated with molecule **1** (50 nM) for 10 min. After extensive washing, the cells were incubated with molecule **3** (500 nM). Pretreatment with molecule **1** impaired the ability of molecule **3** to form a covalent bond with EGFP–TRPA1 (Figure S4). Pretreatment with molecule **2**, a nonelectrophilic analogue of molecule **1**, failed to do so, even at concentrations up to 5 μM (Figure S5). Furthermore, when the cells were pretreated with molecule **3** for 10 min and subsequently incubated with molecule **1**, we observed no detectable effects on the ability of molecule **3** to form a covalent bond with EGFP–TRPA1 (Figure S4). These results support our hypothesis that molecules **1** and **3** form irreversible bonds with EGFP–TRPA1.

Binding Site of Molecule 3. Pretreatment of cells overexpressing EGFP–TRPA1 with AITC, a TRPA1 agonist found in wasabi, also impaired the ability of molecule **3** to form a covalent bond with EGFP–TRPA1, although high concentrations (>25 μM) of AITC were required (Figure S6). This result suggests that the modification sites of molecule **3** overlap those of AITC.

The modification sites of electrophilic agonists, including AITC, have been identified as six cysteine residues in the NH_2 terminal cytosolic segment of TRPA1: Cys414, Cys421, Cys540, Cys621, Cys641, and Cys665.[15,16,21] Cells overexpressing EGFP fusions of TRPA1 mutants, in which one of the six cysteines was replaced with a serine, were incubated with molecule **3** (500 nM), and the effects were analyzed using Western blots. The C621S mutant of TRPA1 was resistant to the modification; all other mutants reacted with molecule **3** at levels comparable to the wild type (Figure 4A). These results suggest that Cys621 is the major binding site of molecule **3**.

To confirm that Cys621 mediates the channel opening induced by molecule **3**, HEK293 cells overexpressing a C621S mutant of TRPA1 were treated with molecule **3**. As expected, the C621S mutant cells were almost completely nonresponsive to molecule **3**, even at 500 nM, while wild type cells exhibited calcium influx in the presence of the same concentration of molecule **3** (Figure 4B and Figure S7). In contrast, the response of the C621S mutant cells to AICT was similar to that of the wild type cells.

Ser mutants of the five other cysteine residues were also examined in a cellular context (Figure 4C). Point mutations at Cys414 or Cys621 exhibited the most pronounced effects on channel opening induced by molecule **3**. Calcium influx levels of the C414S and C621S mutants in the presence of molecule **3** were as low as levels with DMSO, indicating that these two mutants were essentially nonresponsive to molecule **3**. However, the C414S mutant also exhibited little response to AITC. Presumably, Cys414 is generally required for opening the TRPA1 channel. In fact, Cys414 mutants have been shown to be nonresponsive even to 2-APB, a noncovalent TRPA1 agonist.[13,15,21]

When molecule **1** was similarly tested in the C621S mutant cells, molecule **1** (10 nM) failed to stimulate calcium influx in the C621S mutant cells but induced calcium influx in the wild type cells (Figure 4D,E and Figure S8). These results confirm that molecule **1** and **3** activates TRPA1 primarily through covalent modification at Cys621.

Direct Observation of Molecule 3 in TRPA1. Reactive TRPA1 agonists usually stimulate channel opening through modification of multiple cysteine residues.[16] The present study found that molecule **3** is a nanomolar range agonistic probe that opens the TRPA1 channel by binding covalently and selectively to a single cysteine, Cys621. The biotinylated chemical probe can be used as a tool for mechanistic studies of TRPA1.

DOI: 10.1021/jacs.5b10162
J. Am. Chem. Soc. 2015, 137, 15859–15864

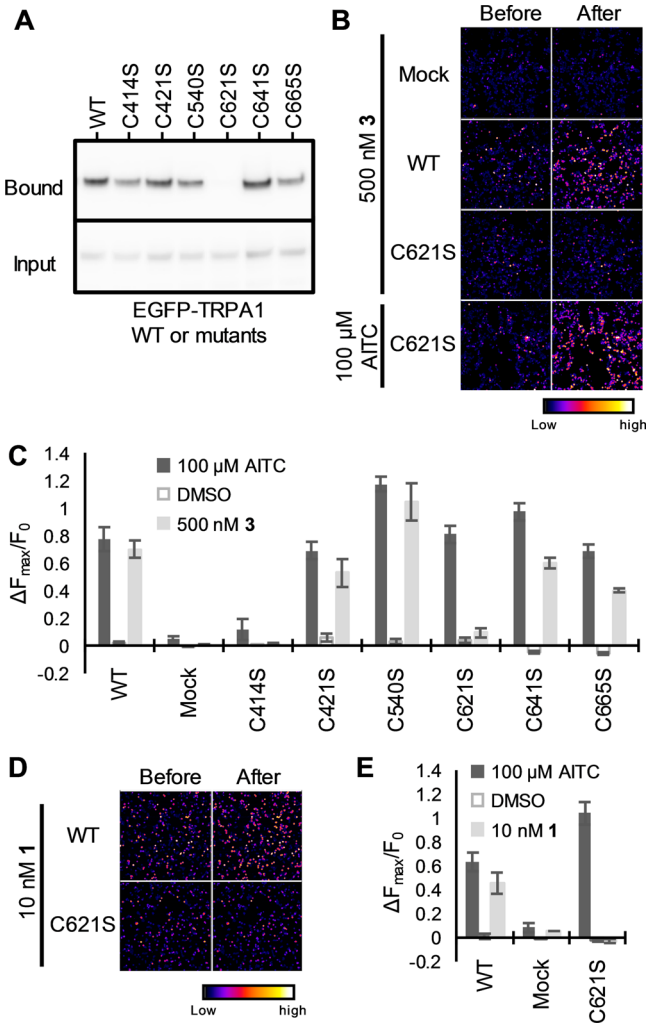

Figure 4. A TRPA1 C621S mutant resists both biotinylation and channel opening induced by molecule **3**. (A) Effect of Cys to Ser mutations. EGFP-TRPA1 wild type (WT)- or mutant (C414S, C421S, C540S, C621S, C641S, or C665S)-transfected HEK293 cells were incubated with molecule **3** (500 nM), and biotinylated proteins were purified using avidin beads and analyzed by Western blot analysis. (B) Representative calcium imaging for response analysis of Fluo-8-loaded WT-, C621S-, or mock-transfected HEK293 cells to molecule **3** or AITC. (C) Effect of the mutations on channel responses to molecule **3**, DMSO control, or AITC. Data points are mean ± s.e.m. (n = 3–20). (D) Representative calcium imaging for response analysis of Fluo-8-loaded WT- or C621S-transfectd HEK293 cells to molecule **1**. (E) Effect of the C621S mutant on channel responses to molecule **1**, DMSO control, or AITC. Data points are mean ± s.e.m. (n = 3–4).

To demonstrate its utility, we carried out electron microscopic visualization of the interaction between TRPA1 and molecule **3**. TRPA1 tagged with FLAG at the COOH terminus was overexpressed in FreeStyle 293-F cells and purified through FLAG affinity chromatography, wheat germ agglutinin (WGA) affinity chromatography, and size-exclusion chromatography (Figure S9A). Blue native-PAGE analysis showed a broad single band at ∼560 kDa (Figure S9B), suggesting that purified FLAG−TRPA1 forms a tetramer, consistent with previously proposed models.[29,30]

The purified FLAG−TRPA1 tetramers were incubated with molecule **3** (5 μM) and streptavidin−gold conjugates (SA−gold). After removal of unreacted molecule **3** and SA−gold by FLAG affinity chromatography, the biotinylation status of FLAG−TRPA1 was confirmed by avidin blot analysis, using streptavidin−HRP (Figure S10A). Electron microscopic observation of the negatively stained sample showed snowman-shaped images comprising two particles: a larger particle (FLAG−TRPA1) and a smaller particle (SA−gold). Comparison of the FLAG−TRPA1 particle images in the presence or absence of molecule **3** (Figure S10B) detected no obvious conformational transition of TRPA1 tetramers due to the relatively low resolution of the images. Based on the size of the black dots resulting from gold nanoparticles (5 nm), the FLAG−TRPA1 tetramer was estimated to be ∼15 nm in diameter (Figure 5A and Figure S10B), which agrees with

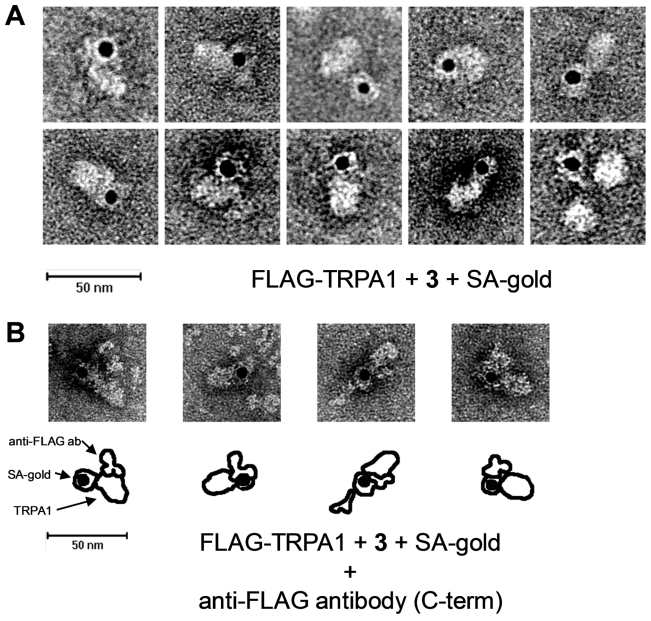

Figure 5. Electron microscopic observation of TRPA1 tetramer biotinylated by molecule **3**. (A) Representative negatively stained images of biotinylated FLAG-TRPA1 tetramer labeled with streptavidin−gold nanoparticle (SA−gold). Purified FLAG−TRPA1 tetramer was incubated with 5 μM molecule **3** for 1 h and then labeled with SA−gold. (B) Estimated orientation of FLAG−TRPA1. The FLAG-tagged COOH terminal end of FLAG−TRPA1 is known to be cytoplasmic. The locations of the FLAG tags were estimated by adding an anti-FLAG antibody to the samples of (A).

previously proposed models.[30] Most of the SA−gold particles were located close to the end of the longer axis of the TRPA1 protein particles, suggesting the location of biotinylated sites in the particles.

To examine the orientation of FLAG−TRPA1 in the images, we treated the sample with an anti-FLAG antibody, which detects a FLAG tag at the cytoplasmic COOH terminus of FLAG−TRPA1 (Figure 5B). Preferred binding of anti-FLAG antibodies to the gold-labeled sides of particles suggested that the biotinylation sites are located in the cytoplasmic component of TRPA1. This observation is consistent with the proposed cytoplasmic location of Cys621.[29,30]

■ DISCUSSION

Results of the present study indicate that the chloroacetamide moiety of molecules **1** and **3** binds covalently and selectively to a single cysteine, Cys621, in TRPA1. The chloroacetamide group is generally known to be a moderately electrophilic

DOI: 10.1021/jacs.5b10162
J. Am. Chem. Soc. 2015, 137, 15859−15864

functional group.[31] In fact, as high as >100 mM of dithiothreitol was required to prevent molecule **3** from reacting with TRPA1 in cells (Figure S11), and only 10% of molecule **1** reacted with 2-mercaptoethanol when incubated at the concentrations of 1 mM for 2 h (data not shown). Molecules **1** and **3** have a mechanism by which they react with Cys621 in TRPA1, in the presence of the abundant thiols and amines in cells.

During the course of our study, Paulsen et al. described a cryo-electron microscopic (Cryo-EM) structure of a TRPA1 tetramer, in which Cys621 is located at the NH_2 terminus of an α-helix and adjacent to a lysine.[30] The dipolar moment of the helix and the basicity of the lysine might reduce the pK_a of the thiol moiety of Cys621, rendering Cys621 more nucleophilic than other cysteine residues. Furthermore, Cys621 is located in a pocket between an ankyrin repeat and an overlying helix-turn-helix. Presumably, the size and shape of the pocket are complementary to molecule **1**, increasing the reactivity of molecule **1** with Cys621 through proximity effects. In fact, the activity of molecule **1** is highly sensitive to modification. For example, screening of the chemical library revealed 73 molecules with a 2-chloro-*N*-(thiazol-2-yl)acetamide structure (Figure S1F), while only three of those molecules exhibited sub-nanomolar activity.

Three-dimensional structural analysis of a ligand−TRPA1 complex is needed for molecular understanding of how the modification of Cys621 with molecule **1** leads to opening of the TRPA1 channel. Such analysis was not possible in the recent Cryo-EM study due to insufficient resolution of AITC-adducted TRPA1 and instability/inefficiency of the AITC adduct formation.[30] Molecule **1** (EC_{50} = 0.65 nM) is >3000-fold more potent than AITC (EC_{50} = 2 μM; Figure S6A). Molecule **1** might prove to be useful for future structural studies of a ligand−channel complex.

Our results suggest that Cys621 is important in channel opening. However, previous studies reported mixed results on the importance of Cys621. NNO-ABBH, a TRPA1-selective NO donor, retained its agonist activity in the C621S mutant,[21] while 15d-PGJ_2, an anti-inflammatory mediator known as the TRPA1 agonist,[32,33] exhibited suppressed channel opening and reduced binding with the C621S mutant.[13] Surprisingly, Moparthi et al. reported that a deletion mutant (Δ1-688 hTRPA1), lacking most of the cysteine residues that are important for electrophilic agonists, maintained its cold- and chemosensitivities.[34] Thus, modification of Cys621 is likely to be sufficient, but not necessary, for opening TRPA1 channel.

EXPERIMENTAL SECTION

Cell Culture. Human embryonic kidney 293 (HEK293) cells were cultured in Dulbecco's modified Eagles' medium (Thermo Fisher Scientific Inc., Waltham, MA), containing 10% fetal bovine serum, 100 units/mL penicillin, 100 μg/mL streptomycin, and 0.25 μg/mL amphotericin B, at 37 °C under 5% CO_2.

Fluorescent Calcium Imaging with Fluo-8. Transfected cells were trypsinized, diluted with DMEM, and plated on poly-D-lysine-coated glass-bottom viewplate-96 F (PerkinElmer Inc., Waltham, MA) at a density of 25 000−30 000 cells/well. 3 to 9 h after plating, the medium was changed to flesh DMEM, containing 4 μM Fluo-8 AM (AAT Bioquest, Inc., Sunnyvale, CA), and the cells were incubated at 37 °C under 5% CO_2 for 1 h. The medium containing Fluo-8 AM was replaced with 200 μL of HEPES-buffered saline, containing the following: 107 mM NaCl, 6 mM KCl, 1.2 mM $MgSO_4$, 2 mM $CaCl_2$, 11.5 mM glucose, and 20 mM HEPES (pH 7.4, adjusted with NaOH). The Fluo-8 fluorescence images were recorded every 5 min, using Cell Voyager CV1000 (Yokogawa Electric Corporation, Tokyo, Japan), a confocal microscope system, with excitation by Ar laser (wavelength, 488 nm), and a 525/50 bandpass filter. Recorded images were analyzed using ImageJ (NIH, Bethesda, MD).

Biotinylation Assay. Transfected cells (3×10^6 cells plated on a 100 mm diameter dish) were collected by scraping and washed twice with PBS. The cells were divided into eight tubes and mixed with or without molecule **3** and other chemicals at various concentrations. After extensive washing with PBS, the cell pellets were suspended in 1 mL of RIPA buffer, containing the following: 150 mM NaCl, 1% Nonidet P-40, 1% sodium deoxycholate, 0.1% SDS in 25 mM Tris-HCl (pH 7.5), and 10 mM DTT with 1× protease inhibitor cocktail (Nacalai Tesque, Inc., Kyoto, Japan). The cell suspensions were sonicated using an ASTRASON W-385 ultrasonic processor (Heat Systems-Ultrasonics, Inc., Newtown, CT) for 10 s and incubated on ice for 30 min. Lysates were centrifuged at 20000*g* for 20 min, and small portions of supernatants were collected as input fractions. Remaining supernatants were mixed with 25 μL of High Capacity NeutrAvidin Agarose Resin (Pierce Biotechnology, Waltham, MA) or SoftLink Soft Release Avidin Resin (Promega Corp., Madison, WI) and incubated at 4 °C for 2−4 h. The resin was washed at least four times with RIPA buffer, and biotinylated samples were eluted from the beads. The High Capacity NeutrAvidin Agarose Resin was incubated with 1× SDS sample buffer, containing 100 mM DTT, at room temperature (RT) for 30 min. The SoftLink Soft Release Avidin Resin was incubated with RIPA buffer, containing 5 mM biotin at RT for 30 min. Eluted samples were collected as the bound fractions and examined by SDS-PAGE analysis in a 4−20% gradient gel (Cosmo Bio, Inc., Tokyo, Japan) and Western blot analysis with Living Colors EGFP Monoclonal Antibody (Clontech Laboratories, Inc., Palo Alto, CA) or an anti-TRPA1 antibody (NB110-40763; Novus Biologicals, LLC, Littleton, CO) diluted with Can Get Signal Immunoreaction Enhancer Solution (Toyobo, Osaka, Japan). The blotted membranes were visualized with ECL Prime Western Blotting Detection Reagent and recorded using ImageQuant LAS500 (GE Healthcare, Little Chalfont, UK).

Electron Microscopic Analysis. Purified FLAG-TRPA1 tetramer was incubated with 5 μM molecule **3** at 4 °C for 1 h. The sample was then incubated with 20 μL of anti-FLAG affinity beads (Sigma-Aldrich) for 1 h. After extensive washing, the beads were incubated with 4 μL of streptavidin−gold nanoparticle conjugate (BBInternational) at 4 °C for 20 min. Unbound SA−gold conjugates were removed by washing the gel. The TRPA1−molecule **3**−SA−gold complex was eluted from the gel with 40 μL of 100 μg/mL FLAG peptide (Sigma-Aldrich). Peptide was removed by Superdex 200 gel filtration chromatography (GE Healthcare) prior to conjugation with anti-FLAG antibodies.

The eluate containing gold-labeled TRPA1 was adsorbed onto thin carbon films supported by copper mesh grids, which were rendered hydrophilic in advance by glow discharge under low air pressure. Samples were washed with five drops of double-distilled water, negatively stained with 2% uranyl acetate solution for 30 s twice, blotted, and dried in air. Samples were observed using a JEM1230 transmission electron microscope (JEOL, Tokyo, Japan) at ×60 000 magnification with 100 kV acceleration voltages. Images were recorded using a TVIPS F114T CCD camera (TVIPS, Oslo, Norway).

ASSOCIATED CONTENT

Supporting Information

The Supporting Information is available free of charge on the ACS Publications website at DOI: 10.1021/jacs.5b10162.

Details on construction of recombinant plasmids, overexpression of recombinant proteins, chemical screening, quantification of Fluo8 fluorescence images, protein purification, synthesis schemes, and molecule characterization data including ^{1}H NMR spectra (PDF)

DOI: 10.1021/jacs.5b10162
J. Am. Chem. Soc. 2015, 137, 15859−15864

AUTHOR INFORMATION

Corresponding Author

*E-mail uesugi@scl.kyoto-u.ac.jp (M.U.).

Notes

The authors declare no competing financial interest.

ACKNOWLEDGMENTS

We thank N. Takahashi and D. Kozai for experimental support. This work was supported in part by JSPS KAKENHI Grants 26102728 and 26220206 (M.U.). iCeMS is supported by World Premier International Research Center Initiative (WPI), MEXT, Japan. This work was inspired by the international and interdisciplinary environments of the iCeMS and JSPS Asian CORE Program, "Asian Chemical Biology Initiative".

ABBREVIATIONS

AITC, allyl isothiocyanate; AP-18, 4-(4-chlorophenyl)-3-methylbut-3-en-2-one oxime; 2-APB, 2-aminoethoxydiphenyl borate; DMSO, dimethyl sulfoxide; DTNP, 2,2′-dithiobis(5-nitropyridine); HC-030031, 2-(1,3-dimethyl-2,6-dioxo-1,2,3,6-tetrahydro-7*H*-purin-7-yl)-*N*-(4-isopropylphenyl)acetamide; SNAP, *S*-nitroso-*N*-acetylpenicillamine; TRP, transient receptor potential.

REFERENCES

(1) Clapham, D. *Nature* **2003**, *426* (6966), 517−24.
(2) Nilius, B.; Owsianik, G.; Voets, T.; Peters, J. *Physiol. Rev.* **2007**, *87* (1), 165−217.
(3) Benemei, S.; Patacchini, R.; Trevisani, M.; Geppetti, P. *Curr. Opin. Pharmacol.* **2015**, *22*, 18−23.
(4) Bessac, B. F.; Sivula, M.; Hehn, C. A.; von Escalera, J.; Cohn, L.; Jordt, S.-E. E. *J. Clin. Invest.* **2008**, *118* (5), 1899−1910.
(5) Bessac, B. F.; Jordt, S.-E. E. *Physiology* **2008**, *23*, 360−70.
(6) Caterina, M. J.; Schumacher, M. A.; Tominaga, M.; Rosen, T. A.; Levine, J. D.; Julius, D. *Nature* **1997**, *389* (6653), 816−824.
(7) Moran, M.; McAlexander, M.; Bíró, T.; Szallasi, A. *Nat. Rev. Drug Discovery* **2011**, *10*, 601−620.
(8) Julius, D. *Annu. Rev. Cell Dev. Biol.* **2013**, *29*, 355−84.
(9) Story, G. M.; Peier, A. M.; Reeve, A. J.; Eid, S. R.; Mosbacher, J.; Hricik, T. R.; Earley, T. J.; Hergarden, A. C.; Andersson, D. A.; Hwang, S. W.; McIntyre, P.; Jegla, T.; Bevan, S.; Patapoutian, A. *Cell* **2003**, *112* (6), 819−29.
(10) Wang, Y.; Chang, R.; Allgood, S.; Silver, W.; Liman, E. *J. Gen. Physiol.* **2011**, *137* (6), 493−505.
(11) Fujita, F.; Uchida, K.; Moriyama, T.; Shima, A.; Shibasaki, K.; Inada, H.; Sokabe, T.; Tominaga, M. *J. Clin. Invest.* **2008**, *118* (12), 4049−4057.
(12) de la Roche, J.; Eberhardt, M.; Klinger, A.; Stanslowsky, N.; Wegner, F.; Koppert, W.; Reeh, P.; Lampert, A.; Fischer, M.; Leffler, A. *J. Biol. Chem.* **2013**, *288* (28), 20280−20292.
(13) Takahashi, N.; Mizuno, Y.; Kozai, D.; Yamamoto, S.; Kiyonaka, S.; Shibata, T.; Uchida, K.; Mori, Y. *Channels* **2008**, *2* (4), 287−98.
(14) Hu, H.; Bandell, M.; Petrus, M.; Zhu, M.; Patapoutian, A. *Nat. Chem. Biol.* **2009**, *5* (3), 183−90.
(15) Hinman, A.; Chuang, H.; Bautista, D.; Julius, D. *Proc. Natl. Acad. Sci. U. S. A.* **2006**, *103* (51), 19564−19568.
(16) Macpherson, L.; Dubin, A.; Evans, M.; Marr, F.; Schultz, P.; Cravatt, B.; Patapoutian, A. *Nature* **2007**, *445* (7127), 541−5.
(17) Bautista, D.; Movahed, P.; Hinman, A.; Axelsson, H.; Sterner, O.; Högestätt, E.; Julius, D.; Jordt, S.-E.; Zygmunt, P. *Proc. Natl. Acad. Sci. U. S. A.* **2005**, *102* (34), 12248−12252.
(18) Jordt, S.-E. E.; Bautista, D. M.; Chuang, H.-H. H.; McKemy, D. D.; Zygmunt, P. M.; Högestätt, E. D.; Meng, I. D.; Julius, D. *Nature* **2004**, *427* (6971), 260−5.
(19) Petrus, M.; Peier, A.; Bandell, M.; Hwang, S.; Huynh, T.; Olney, N.; Jegla, T.; Patapoutian, A. *Mol. Pain* **2007**, *3*, 40.
(20) McNamara, C.; Mandel-Brehm, J.; Bautista, D.; Siemens, J.; Deranian, K.; Zhao, M.; Hayward, N.; Chong, J.; Julius, D.; Moran, M. *Proc. Natl. Acad. Sci. U. S. A.* **2007**, *104* (33), 13525−13530.
(21) Kozai, D.; Kabasawa, Y.; Ebert, M.; Kiyonaka, S.; Firman; Otani, Y.; Numata, T.; Takahashi, N.; Mori, Y.; Ohwada, T. *Mol. Pharmacol.* **2014**, *85*, 175−185.
(22) Yoshida, T.; Inoue, R.; Morii, T.; Takahashi, N.; Yamamoto, S.; Hara, Y.; Tominaga, M.; Shimizu, S.; Sato, Y.; Mori, Y. *Nat. Chem. Biol.* **2006**, *2* (11), 596−607.
(23) Sawada, Y.; Hosokawa, H.; Matsumura, K.; Kobayashi, S. *Eur. J. Neurosci.* **2008**, *27* (5), 1131−42.
(24) Hara, Y.; Wakamori, M.; Ishii, M.; Maeno, E.; Nishida, M.; Yoshida, T.; Yamada, H.; Shimizu, S.; Mori, E.; Kudoh, J.; Shimizu, N.; Kurose, H.; Okada, Y.; Imoto, K.; Mori, Y. *Mol. Cell* **2002**, *9* (1), 163−173.
(25) Macpherson, L. J.; Hwang, S. W.; Miyamoto, T.; Dubin, A. E.; Patapoutian, A.; Story, G. M. *Mol. Cell. Neurosci.* **2006**, *32* (4), 335−43.
(26) Everaerts, W.; Gees, M.; Alpizar, Y.; Farre, R.; Leten, C.; Apetrei, A.; Dewachter, I.; van Leuven, F.; Vennekens, R.; De Ridder, D.; Nilius, B.; Voets, T.; Talavera, K. *Curr. Biol.* **2011**, *21* (4), 316−321.
(27) Uchida, K.; Miura, Y.; Nagai, M.; Tominaga, M. *Chem. Senses* **2012**, *37* (9), 809−818.
(28) Terada, Y.; Masuda, H.; Watanabe, T. *J. Nat. Prod.* **2015**, *78* (8), 1937−41.
(29) Cvetkov, T.; Huynh, K.; Cohen, M.; Moiseenkova-Bell, V. *J. Biol. Chem.* **2011**, *286* (44), 38168−38176.
(30) Paulsen, C. E.; Armache, J.-P. P.; Gao, Y.; Cheng, Y.; Julius, D. *Nature* **2015**, *520* (7548), 511−7.
(31) Weerapana, E.; Simon, G.; Cravatt, B. *Nat. Chem. Biol.* **2008**, *4*, 405−407.
(32) Taylor-Clark, T.; Undem, B.; Macglashan, D.; Ghatta, S.; Carr, M.; McAlexander, M. *Mol. Pharmacol.* **2007**, *73* (2), 274−281.
(33) Cruz-Orengo, L.; Dhaka, A.; Heuermann, R.; Young, T.; Montana, M.; Cavanaugh, E.; Kim, D.; Story, G. *Mol. Pain* **2008**, *4*, 30.
(34) Moparthi, L.; Survery, S.; Kreir, M.; Simonsen, C.; Kjellbom, P.; Högestätt, E.; Johanson, U.; Zygmunt, P. *Proc. Natl. Acad. Sci. U. S. A.* **2014**, *111* (47), 16901−16906.

DOI: 10.1021/jacs.5b10162
J. Am. Chem. Soc. 2015, 137, 15859−15864